SLAC-PUB-5610
August 1991
T/E

The Photon Distribution of Atoms and Molecules

MATTHIAS BURKARDT,*

Stanford Linear Accelerator Center

Stanford University, Stanford, California 94309

ABSTRACT

In the weak coupling limit of QED, it is shown how to express the parton distributions — in particular the photon distribution — in terms of the nonrelativistic wavefunctions. A sum rule is derived, relating the momentum carried by the photons to the binding energy, thus allowing quantitative predictions about the modification of the photon distribution as molecules are formed from atoms. The physical content is illustrated in a semi-classical picture as well as by providing analytic results for positronium.

Submitted to *Nuclear Physics B*

* Supported in part by a grant from Alexander von Humboldt-Stiftung and in part by the Department of Energy under contract DE-AC03-76SF00515.

1. INTRODUCTION

In the near future, more precise data on the total momentum carried by quarks in nucleons and nuclei will become available[1]. Using momentum conservation, one will thus be able to extract the fraction of the hadron's momentum which is carried by the QCD gauge field. Therefore, at least in principle, one can measure the change in the gluon momentum when nuclei are formed out of individual nucleons.

Another type of experiment to extract information about gluon distributions in the nucleon is the inclusive photoproduction of charmed hadrons[2], where the $\gamma g \rightarrow c\bar{c}$ subprocess is used as an indirect tool to obtain information on spin and momentum distribution of the gluons.

On the theoretical side, very little is known about gluon distributions beyond perturbation theory. In particular, in the low x_{Bj} region, soft processes and/or interference effects might be very important for the dynamics of long wavelength gluons[3]. In this regime, hadronic size effects as well as nuclear binding (with possible associated scale changes) could affect the gluon distributions[4] . Because of the complexity of the problem of calculating such distributions in QCD, I will not directly attempt to make predictions about gluon distributions but rather focus on a similar but much simpler and, as we will see in the following sections, nevertheless quite interesting problem. To get intuition about what matters in such computations, we will study the photon distributions in weak coupling QED (distributions in the sense of parton-distributions). In a first approximation QED for small coupling corresponds to solving the Schrödinger equation of the corresponding Coulomb problem. In this article, we will go one step further and allow for dynamical photons. This will be done in the context of the light-front form of dynamics for QED[7,6,5,8,9]. By expanding the Fock space around the Schrödinger

solution, information about the photon component of the wave function can be obtained (see also Ref.3). Since the internal motion in the rest frame of a weakly coupled bound state is essentially nonrelativistic, one can relate the photon distributions to the corresponding nonrelativistic wave functions. The resulting distributions are then subject of the rest of the article, where the main focus will be on developing an intuitive understanding for general properties of low x photons. Naturally, in bound systems, this includes atomic and molecular size effects as well as atomic and molecular binding strengths. A key result of the light-cone momentum distributions of photons is a sum rule that relates atomic and molecular binding energies to the momentum carried by the photon field. Another sum rule will be obtained, that relates the transverse size of positronium states to the $x \to 0$ limit of the photon distributions. The photon distributions, as well as the sum rules will be illustrated in the quasi-classical limit, as well as by performing explicit computations in the positronium system.

2. Photon Distributions for Weak Coupling

The technique to be used in this work to compute the photon distributions in QED-bound states is based on a Fock-space expansion at equal light-cone time $\tau = t + x$ in the light-cone gauge $A^+ = A^0 + A^1 = 0$[5,8]. This approach allows to represent the parton distributions in a given state in terms of squares of Fock-space amplitudes[3], i.e. in a form which should be familiar from nonrelativistic many-body theory. This very physical approach to a relativistic quantum theory is explained in more detail in Ref. 10 , where the relevant definitions can be found.[#1]

#1 There are numerous studies under way to investigate similar problems for general values

For small α only two Fock-space amplitudes will be relevant: the valence configuration (no photons present) and the state with one additional photon[#2]. Furthermore, consistent with the one-photon approximation, interactions arising from instantaneous photon exchange in the excited $(e^+e^-\gamma)$ Fock-component are dropped[5,8]. Using these approximations, it has been shown in Ref.3 that one can express the photon distribution $G(x,k_\perp)$ entirely in terms of the valence amplitudes. For example, in the case of positronium one finds[3] for the unpolarized photon distribution[#3] (here and in the following, vector arrows on perpendicular momenta are omitted for notational convenience)

$$G(x,k_\perp) = \frac{\alpha}{\pi^2}\int d^2l_\perp \int_x^1 dy \left\{ \left[\psi(y,l_\perp)\frac{yk_\perp - xl_\perp}{y-x} - \psi(y-x,l_\perp-k_\perp)\frac{(1-y)k_\perp + xl_\perp}{1-y}\right]^2 \frac{1}{x^3} \right.$$
$$+ |\psi(y,l_\perp)|^2 \frac{xm^2}{(y-x)^2y^2} + |\psi(y-x,l_\perp-k_\perp)|^2 \frac{xm^2}{(1-y)^2[1-(y-x)]^2}$$
$$\left. + \left[\psi(y,l_\perp)\frac{yk_\perp - xl_\perp}{y} - \psi(y-x,l_\perp-k_\perp)\frac{(1-y)k_\perp + xl_\perp}{1-(y-x)}\right]^2 \frac{1}{x^3} \right\} \frac{1}{D^2} \tag{1}$$

where

$$D = M_B^2 - \frac{(l_\perp - k_\perp)^2 + m^2}{y-x} - \frac{l_\perp^2 + m^2}{1-y} - \frac{k_\perp^2}{x}. \tag{2}$$

Here m and M_B are the electron and bound state masses respectively. x and y

---

of α[7,6,5,8,9]. Since we will work exclusively in the weak coupling it won't be necessary to introduce the whole formalism here. For more details, as well as for a discussion of the problems associated with the light-cone formalism[11] we refer to these works and references therein.

#2 Since we will deal with charge neutral systems only there are no problems arising from infrared divergences that might spoil the perturbative arguments[3]. UV-divergences are taken care of by working with a fixed cutoff.

#3 Hyperfine splitting effects and the associated polarization of the photon structure function are higher order in α effects and will not be considered here.

are the longitudinal momentum fractions carried by the photon and electron. The wavefunctions and distributions are normalized such that $\int d^2l_\perp \int_0^1 dy|\psi(y,l_\perp)|^2 = 1$. Then $\int d^2k_\perp \int_0^1 dx x G(x,k_\perp)$ is the momentum fraction carried by the gluons.

In the following we will work in leading order in α. Although this will lead to expressions which look familiar from nonrelativistic (NR) quantum mechanics or which involve the NR wavefunction in the rest frame of the positronium system, the entire calculation will nevertheless be fully relativistic and exact to leading order in α.[#4] In this limit, the e^+e^--component of the positronium wavefunction $\psi(y,l_\perp)$ is sharply peaked around $y=\frac{1}{2}$ and one finds (for $y=\frac{1}{2}+\mathcal{O}(\alpha)$, $l_\perp^2=\mathcal{O}(m^2\alpha^2)$)

$$\psi(y,l_\perp) = \sqrt{2m}\psi_{NR}\left(l_L = 2m(y-\frac{1}{2}), l_\perp\right) \tag{3}$$

(here the longitudinal momentum $l_L = 2m(y-\frac{1}{2})$ has been expressed in terms of the light-cone momentum fraction y). Thus for the ground state of positronium[10]

$$\psi^{1s}(y,l_\perp) = \frac{1}{m\alpha^{\frac{3}{2}}\pi\sqrt{2}} \frac{1}{\left(\left[\frac{2}{\alpha}(y-\frac{1}{2})\right]^2 + \left(\frac{l_\perp^2}{m\alpha}\right)^2 + \frac{1}{4}\right)^2}. \tag{4}$$

In the Appendix A such relations will be used to calculate the various parton distributions for the lowest lying positronium states.

The photon distribution can be divided up into a piece associated with self-interactions, which contains $|\psi(y,l_\perp)|^2$ or $|\psi(y-x,l_\perp-k_\perp)|^2$, and an interaction piece, containing the interference term $\psi(y,l_\perp)\psi^*(y-x,l_\perp-k_\perp)+c.c.$. Using

#4 For most purposes the difference between NR and weak coupling approximation is irrelevant. However, there is at least one important distinction that arises if one wants to use the wavefunctions thus obtained for the calculation of relativistic processes — in particular deep inelastic scattering in order to measure these parton distributions — which is, strictly speaking, no longer possible once one has performed the NR limit.

$M_B^2 = (2m)^2 + \mathcal{O}(\alpha^2)$ and $y = \frac{1}{2} + \mathcal{O}(\alpha)$ one finds for the photon distribution arising from the emission and absorption of the photon from the same particle ($x = \mathcal{O}(\alpha)$, sum of e^+e^--contribution)

$$G^{self}(x) \equiv \int d^2k_\perp \theta(\Lambda_\perp^2 - k_\perp^2) G^{self}(x, k_\perp) \tag{5}$$

with

$$xG^{self}(x, k_\perp) = \frac{2\alpha}{\pi^2} \frac{k_\perp^2}{\left[k_\perp^2 + (2mx)^2\right]^2} + \mathcal{O}(\alpha^2), \tag{6}$$

hence

$$xG^{self}(x) = \frac{2\alpha}{\pi} \left[\ln \left(\frac{\left(\frac{\Lambda_\perp}{m\alpha}\right)^2}{\left(\frac{2x}{\alpha}\right)^2} \right) - 1 \right] + \mathcal{O}(\alpha^2) + \mathcal{O}((\frac{Mx}{\Lambda_\perp})^2), \tag{7}$$

where a transverse momentum cutoff $\Lambda_\perp$ has been introduced (implicitly the photon distributions will thus be cutoff dependent). Hereafter all corrections of order $\mathcal{O}(\frac{1}{\Lambda_\perp^2})$ will be dropped. Note that this result is independent of the bound state wavefunction and mass, i.e. it is equal to the photon distribution around a free electron and positron with momentum fraction $y = \frac{1}{2}$.[#5]

For the interaction term one finds (Fig. 1.)

$$xG^{int}(x, k_\perp) = -\frac{\alpha}{\pi^2} \frac{k_\perp^2}{\left[k_\perp^2 + (2mx)^2\right]^2} \int d^2l_\perp \int_x^1 dy \left[\psi(y, l_\perp)\psi^*(y - x, l_\perp - k_\perp) + c.c.\right]. \tag{8}$$

In the case of positronium[#6] one can express this result in terms of an expression

---

#5 Eq.(6)is correct only for $x = \mathcal{O}(\alpha)$. However, the correct expression for larger values of x will also be independent of the bound state wavefunction and binding energies and thus drops out when different states with the same valence content are compared.

#6 For systems with more than two valence particles this is no longer possible.

that looks like an elastic form factor $F(\vec{k})$ using (3)

$$\int d^2l_\perp \int dy\,[\psi(y,l_\perp)\psi^*(y-x,l_\perp-k_\perp)+c.c.] = \int d^3\vec{l}[\psi_{NR}(l_L,l_\perp)\psi^*_{NR}(l_L-k_L,l_\perp-k_\perp)+c.c.] = 2F(k_L,k_\perp), \tag{9}$$

where we used $k_L = 2m(x-\frac{1}{2})$. The cancellation of the various IR-singularities can be seen most clearly by considering[3]

$$G^{total}(x,k_\perp) \equiv G^{self}(x,k_\perp) + G^{int}(x,k_\perp). \tag{10}$$

One finds the compact expression for the photon distribution in the $e^+e^-\gamma$ component of positronium (Fig. 2.)

$$G^{total}(x,k_\perp) = \frac{\alpha}{\pi^2}\frac{\frac{k_\perp^2}{x}}{\left[k_\perp^2+(2mx)^2\right]^2}\int d^2l_\perp \int_x^1 dy|\psi(y,l_\perp)-\psi^*(y-x,l_\perp-k_\perp)|^2. \tag{11}$$

This result for positronium exhibits most of the general features of photon distributions in electromagnetically bound systems. For example, it turns out that $xG^{tot}(x)$ is finite for $x\to 0$[3]

$$\lim_{x\to 0} xG^{total}(x) = \frac{\alpha}{\pi^2}\int \frac{d^2k_\perp}{k_\perp^2}\theta(\Lambda_\perp^2-k_\perp^2)\int d^2l_\perp \int_0^1 dy|\psi(y,l_\perp)-\psi(y,l_\perp-k_\perp)|^2$$
$$= \frac{2\alpha}{\pi}\left\langle \ln\left[(\vec{r}_{e^+}-\vec{r}_{e^-})_\perp^2\Lambda_\perp^2\right]\right\rangle. \tag{12}$$

Notice that the divergent UV-behaviour of this expression implies a logarithmic dependence on the cutoff. Suppose one uses an invariant mass cutoff, like $\theta(\Lambda^2-D)$, instead. In the small x-region the argument of the θ-function can be effectively

replaced by $x\Lambda^2 - k_\perp^2$, which has the same effect as the cutoff used in (12) but with $\Lambda_\perp^2 = x\Lambda^2$. Thus a $\ln \frac{1}{x}$ divergence would then also appear in in Ee. (12). In the following the simpler $k_\perp$-cutoff (5) will be used throughout.

The generalization of this formalism to general atomic systems with more than two charged particles and unequal masses is straightforward, yielding

$$xG^{self}(x, k_\perp) = \frac{\alpha}{\pi^2} \frac{k_\perp^2}{\left[k_\perp^2 + (Mx)^2\right]^2} \sum_i e_i^2 \tag{13}$$

$$xG^{int}(x, k_\perp) = \frac{\alpha}{\pi^2} \frac{k_\perp^2}{\left[k_\perp^2 + (Mx)^2\right]^2} \int d^2 l_\perp \int dy$$
$$\sum_{i \neq j} e_i e_j \psi(y_i, y_j, l_{i\perp}, l_{j\perp}) \psi^*(y_i - x, y_j + x, l_{i\perp} - k_\perp, l_{j\perp} + k_\perp), \tag{14}$$

where

$$M = \sum_i m_i \tag{15}$$

is the total mass of the system (at leading order in α one can neglect binding for the total mass).[#7] The summation runs over particles and e_i are the charges in units of the electron charge.

For neutral systems, $\sum_i e_i = 0$, hence $\sum_{i \neq j} e_i e_j = -\sum_i e_i^2$, the sum of G^{self}

#7 One might be surprised to find M (15), the total invariant mass of the system, in an expression for the photon distribution arising from self-energy graphs, which (to leading order in α) should not be affected by binding effects. The reason is purely kinematic. For an electron with momentum fraction 1, only its own mass would appear in the denominator of the expression for the photon distribution, but, sine all constituents have about the same average velocity, they carry a mean momentum fraction of $y_i = \frac{m_i}{M}$, which explains the appearance of M in (13).

and G^{total} can be rewritten in the form

$$xG^{total}(x,k_\perp) = -\frac{\alpha}{\pi^2}\frac{k_\perp^2}{\left[k_\perp^2+(Mx)^2\right]^2}\int d^2l_\perp \int dy$$
$$\sum_{i<j} e_i e_j \left[\psi(y_i,y_j,l_{i\perp},l_{j\perp}) - \psi(y_i-x,y_j+x,l_{i\perp}-k_\perp,l_{j\perp}+k_\perp)\right]^2 . \tag{16}$$

For convenience, only those momentum variables (here: labeled i and j), which actually change during the photon exchange process, have been displayed.

The generalization of Eq.(12) to more than two particles reads

$$\lim_{x\to 0} xG^{total}(x) = -\frac{2\alpha}{\pi}\sum_{i<j} e_i e_j \left\langle \ln\left[(\vec{r}_i-\vec{r}_j)_\perp^2\Lambda_\perp^2\right]\right\rangle . \tag{17}$$

As was already mentioned above, these formulae are correct (to order α) only for $x = \mathcal{O}(\frac{\alpha m}{M})$ and $k_\perp = \mathcal{O}(\alpha m)$. However, large $k_\perp$ photons are important only for the self-energy (extrinsic) cloud of the charged particles since large momentum transfers in the interaction term are suppressed by wavefunction effects. Since the self-energy cloud of the constituents is (for small α) not affected by binding, the error at large $x = \mathcal{O}(1)$ cancels out if one compares similar atomic or molecular systems A and B, and the resulting $\Delta G(x) = G_A(x) - G_B(x)$ is correct, even for large x.

3. THE PHOTON MOMENTUM SUM RULE

In the following we will evaluate the total momentum fraction of atoms carried by the photons. As a typical example we will consider a hydrogen-like system, i.e. the two body problem with opposite charges and — to keep the discussion general — unequal masses. In order to discuss some interesting phenomena which appear in confining theories as well we will work in $D_\perp$ transverse dimensions.[#8] One can also use this device as a regulator, but this is not the purpose here. For $D_\perp \to 2$ we will use the $k_\perp$ cutoff. Using (8), one finds for the photon momentum arising from the interactions in state A

$$\langle x_\gamma \rangle_A^{int} = \int_0^1 dx x \int d^{D_\perp} k_\perp G_A^{int}(x, k_\perp)$$

$$= -2\alpha \int_0^1 dx \int d^{D_\perp} k_\perp \frac{k_\perp^2}{\left[k_\perp^2 + (xM)^2\right]^2} \int_x^1 dy \int \frac{d^{D_\perp} l_\perp}{\pi^{D_\perp}} \psi_A(y, l_\perp) \psi_A^*(y - x, l_\perp - k_\perp) \tag{18}$$

(in $D_\perp$ dimensions, we choose $\alpha = \frac{e^2}{\pi 2^{D_\perp}}$). If the atom A is an $l = 0$ state, the form factor on the r.h.s. of (18),

$$F_A(x, k_\perp) = \int dy \int d^{D_\perp} l_\perp \psi_A(y, l_\perp) \psi_A^*(y - x, l_\perp - k_\perp), \tag{19}$$

[#9] is immediately rotational invariant, i.e.

$$F_A(x, k_\perp) = F_A\left((xM)^2 + k_\perp^2\right). \tag{20}$$

In the general case (with $l \neq 0$) one first sums over polarization states in (18)

#8 Note that the QED interactions confine charged particles for $D_\perp \leq 1$.

#9 Note that the integration bounds in (19) have not been specified, but we will assume integration from $-\infty$ to ∞ and $\psi(y, l_\perp)$ is assumed to vanish for y outside $[0, 1]$. Actually, for weak coupling such distinctions are irrelevant, since ψ is extremely localized (3).

and then applies the argument of rotational invariance as well. The virtue of a rotational invariant form factor (19) is that this allows to replace

$$k_\perp^2 \to \frac{D_\perp}{D_\perp + 1}\left[k_\perp^2 + (xM)^2\right] \tag{21}$$

in the numerator of Eq. (18), yielding

$$\langle x_\gamma \rangle_A^{int} = -2\alpha \frac{D_\perp}{D_\perp + 1} \int_0^1 dx \int \frac{d^{D_\perp} k_\perp}{k_\perp^2 + (xM)^2} \int_x^1 dy \int \frac{d^{D_\perp} l_\perp}{\pi^{D_\perp}} \psi_A(y, l_\perp)\psi_A^*(y-x, l_\perp - k_\perp). \tag{22}$$

A comparison of Eq. (22) with the expectation value of the light-cone potential energy due to photon exchange[10] for weak coupling,

$$\left\langle V^{LC} \right\rangle_A^{int} = -2M^2\alpha \int_0^1 dx \int \frac{d^{D_\perp} k_\perp}{k_\perp^2 + (xM)^2} \int_x^1 dy \int \frac{d^{D_\perp} l_\perp}{\pi^{D_\perp}} \psi_A(y, l_\perp)\psi_A^*(y-x, l_\perp - k_\perp), \tag{23}$$

shows a remarkable similarity which leads to a number of results. Consistent with the weak coupling approximation, one can express $\langle V^{LC} \rangle$ in terms of the expectation value of the NR Coulomb interaction. If M_A is the invariant mass of the bound state one can write

$$M_A^2 = \left\langle T^{LC} \right\rangle_A + \left\langle V^{LC} \right\rangle_A, \tag{24}$$

where $\langle T^{LC} \rangle_A = M^2 + \mathcal{O}(\alpha^2)$ is the expectation value of the light-cone kinetic energy, but also

$$M_A = M + \left\langle T^{NR} \right\rangle_A + \left\langle V^{NR} \right\rangle_A, \tag{25}$$

where T^{NR} and V^{NR} are the NR kinetic and potential energy respectively. Com-

paring (24) and (25) yields, up to order $\mathcal{O}(\alpha^2)$,

$$\left\langle T^{LC} \right\rangle = M^2 + 2M \left\langle T^{NR} \right\rangle \tag{26}$$

and

$$\left\langle V^{LC} \right\rangle = 2M \left\langle V^{NR} \right\rangle, \tag{27}$$

which implies[#10][#11]

$$\langle x_\gamma \rangle_A^{int} = \frac{2D_\perp}{D_\perp + 1} \frac{\langle V^{NR} \rangle_A}{M}. \tag{28}$$

Obviously, $\langle x_\gamma \rangle_A^{int}$ is always negative, as is $\langle V_{NR} \rangle_A^{int}$ (if we restrict ourselves to electromagnetically bound states). But this should not come as a surprise, since we have omitted the photons arising from self energy processes so far. Including those effects, one obtains of course $\langle x_\gamma \rangle_A^{total} = \langle x_\gamma \rangle_A^{int} + \langle x_\gamma \rangle_A^{self} > 0$. Notice that the self energy pieces will cancel when one compares states with the same valence content (like two H-atoms versus one H_2 molecule). In the next section this point will be discussed in a little more detail from a semi-classical point of view.

We will now turn our attention to discussing the impact of the sum rule (28) on molecular structure functions. The idea will be to compare $\langle x_\gamma \rangle$ in molecules with $\langle x_\gamma \rangle$ in atoms and to investigate the role of molecular binding in this context. In order to keep the discussion as general as possible we introduce the NR Coulomb

---

#10 For more complicated systems, i.e. more than two valence particles, the same relation holds where M is then the sum of all constituent masses.

#11 The same factor $\frac{4}{3}$ which one obtains for $D_\perp = 2$, appears in the relation between energy and momentum if one tries to give mass and momentum of an electron a purely electromagnetic origin.[15] See also section 4.

interaction for arbitrary $D_\perp$ which gives rise to a power law potential of the form

$$V_{NR} \propto \sum_{i<j} e_i e_j |\vec{r}_i - \vec{r}_j|^{1-D_\perp}. \tag{29}$$

The nonrelativistic virial theorem

$$2\left\langle T^{NR}\right\rangle = \sum_i \left\langle \vec{r}_i \cdot \vec{\nabla}_i V\right\rangle \tag{30}$$

thus implies (using $T^{NR} + V^{NR} = E^{NR}$)

$$E^{NR} = \frac{3 - D_\perp}{2}\left\langle V^{NR}\right\rangle. \tag{31}$$

For $D_\perp < 3$ (the physically interesting cases) E^{NR} and $\left\langle V^{NR}\right\rangle$ always have the same sign — whether or not one has confinement ($D_\perp \lesssim 1$). Thus, on a qualitative level, one does not have to differentiate between these two cases in the following discussion.[#12]

Inserting (31) into (28) and comparing two states A and B with the same valence particle content one finds[#13]

$$\langle x_\gamma\rangle_A - \langle x_\gamma\rangle_B = \left(\frac{2D_\perp}{D_\perp + 1}\right)\left(\frac{2}{3 - D_\perp}\right)\frac{E_A^{NR} - E_B^{NR}}{M} \tag{32}$$

(the self-energy photons cancel in Eq.(32)). Note also that the mass M is the same for A and B to leading order in α. Eq.(32) has important consequences if we

---

#12 For the fermion kinetic energy one would have to, since there is a sign change in the analog to (31).

#13 Although this should be clear from the derivation of (28), it should be emphasized that taking average over polarization states is always implied. In fact, in the Appendix A it will be shown that this is indeed necessary for the $n = 2, l = 1$ states of positronium.

compare two atoms (or small molecules) with a bound state of these fragments. Assuming that the fragments do actually bind, which implies $E^{NR}_{two\,atoms} > E^{NR}_{molecule}$, one will always find

$$\langle x_\gamma \rangle_{two\,atoms} > \langle x_\gamma \rangle_{molecule}\,, \tag{33}$$

or, if A^* is an excited state of A (i.e. $0 > E_{A^*} > E_A$)

$$\langle x_\gamma \rangle_A < \langle x_\gamma \rangle_{A^*}\,. \tag{34}$$

It is instructive to point out an important difference between QED and a Yukawa theory with massless (abelian) bosons. For the momentum sum rule (28) the crucial difference arises from the fact that like charges repel each other in QED whereas, if two fermions couple with the same sign to the scalar boson, they will attract each other. Essentially this means that there is destructive interference between self-energy and exchange bosons in a QED-bound state whereas there is constructive interference in the scalar Yukawa theory. Thus, while stronger binding implies less momentum carried by the bosons in QED, the opposite is true for scalar Yukawa. A derivation, similar to the one performed above, yields for the momentum fraction carried by massless scalar bosons (in states bound by the exchange of these scalar bosons) for weak coupling

$$\langle x_{scalar} \rangle_A - \langle x_{scalar} \rangle_B = -\left(\frac{2}{D_\perp + 1}\right)\left(\frac{2}{3 - D_\perp}\right)\frac{E^{NR}_A - E^{NR}_B}{M}, \tag{35}$$

where the nonrelativistic virial theorem (30) has again been applied.

4. Classical Interpretation

The main focus of this section will be on a semi-classical interpretation of several aspects and results in this work. Being the most important result, the momentum sum rule (28) will be discussed first but later we will proceed to a discussion of the interpretation of self-energies.

Let us consider a classical charge distribution with associated electric field $\vec{\mathcal{E}}(\vec{r},t)$. Consistent with our weak coupling expansion, the internal motion of the charges can be assumed to be nonrelativistic, which implies $\vec{\mathcal{B}} \approx 0$ in the rest frame of the system and the total electromagnetic energy (including self-energies) reads

$$E^{EM}_{rest\,frame} = \frac{1}{2}\int d^3\vec{r}\left\langle \vec{\mathcal{E}}(\vec{r})^2 \right\rangle_t , \tag{36}$$

where $\langle\rangle_t$ means: taking time average. If the system is boosted to ultra-relativistic velocity $\vec{v}$ one finds ($\perp$ and $\parallel$ always refer to the direction of $\vec{v}$)

$$\vec{\mathcal{E}}'_\perp = \gamma\left[\vec{\mathcal{E}}_\perp + (\vec{v}\times\vec{\mathcal{B}})_\perp\right] = \gamma\vec{\mathcal{E}}_\perp \tag{37}$$

$$\mathcal{E}'_\parallel = \mathcal{E}_\parallel \ll |\vec{\mathcal{E}}'_\perp| \tag{38}$$

$$\vec{\mathcal{B}}'_\perp = \gamma\left[\vec{\mathcal{B}}_\perp - (\vec{v}\times\vec{\mathcal{B}})_\perp\right] = -(\vec{v}\times\vec{\mathcal{B}})_\perp \tag{39}$$

$$\mathcal{B}'_\parallel = \mathcal{B}_\parallel = 0, \tag{40}$$

with $\gamma^2 = 1-\vec{v}^2$, i.e. an observer at rest finds for the Poynting momentum[14]

$$\vec{P}_\parallel = \gamma^2\int d^3\vec{r}\left\langle \vec{\mathcal{E}}_\perp \times (\vec{v}\times\vec{\mathcal{E}}_\perp\right\rangle_t = \gamma^2\vec{v}\int d^3\vec{r}\left\langle \vec{\mathcal{E}}_\perp^2\right\rangle_t . \tag{41}$$

Taking the Lorentz contraction in the integration measure into account, and using rotational symmetry for expectation values in the rest frame, for example $\langle\mathcal{E}_i^2\rangle =$

$\frac{1}{3}\left\langle \vec{\mathcal{E}}^2 \right\rangle$, one concludes that the fraction

$$\langle x_\gamma \rangle = \frac{\int d^3\vec{r} \left\langle \vec{\mathcal{E}}_\perp^2 \right\rangle_t}{M} = \frac{2}{3} \frac{\int d^3\vec{r} \left\langle \vec{\mathcal{E}}^2 \right\rangle_t}{M} = \frac{4}{3} \frac{E^{EM}_{rest\ frame}}{M} \tag{42}$$

of the total momentum is carried by the electromagnetic field — which is nothing but the classical analog to (28).

From the classical point of view it is quite easy to understand how binding can decrease the momentum carried by effective photons (which is the classical analog to virtual photons). For example if one compares various positronium states: stronger binding implies smaller size and, because of screening, less space is filled with electric field. In particular, if one would give the electron a finite extension (which we do after all if we introduce a cutoff), there is no electric field left over when the electron and the positron sit on top of each other, hence no effective photons.#14

The self-energy component of the photon distribution plays a role similar to the mass renormalization, in the sense that it separates from the bound state dynamics. But it should nevertheless be included into the computation of photon distributions (at least the finite, x-dependent part) since it changes the IR-behaviour of the distributions and thus reflects the screening of the long range tail of the electric field in a bound state. The renormalization aspect is reflected in the sign of the "intrinsic" component of the momentum fraction carried by the photons. For this purpose one recalls how a positive field energy density, like (36), can give rise to the negative potential energy in hydrogen. Of course the total electric field energies of

#14 Notice the difference to the Yukawa theory with scalar bosons. Since attraction occurs between particles that have the same sign in the coupling constant, there won't be screening in the corresponding hydrogen atom.

a proton, an electron as well as the composite object — the hydrogen atom — are positive. One obtains the negative potential energy by subtracting the self energies of electron and positron from the (positive) field energy of the hydrogen system and obtains a negative energy. Similarly, if one renormalizes the photon distribution of positronium, by subtracting the photon distribution of its constituents one obtains negative distributions and "negative momentum fractions".

This subject brings us close to our next subject, namely whether or not to include the self-energy photons into the virtual photon distribution of positronium, i.e. whether one should separate extrinsic (self-energy) and intrinsic (photon exchange) photons 3. The point is that it is in a sense not entirely consistent to take the self-energy (extrinsic[3]) photons into account in the weak coupling limit, since the weak coupling equation of motion consists of the Schrödinger equation where all self-energy interactions are absorbed into a redefinition of masses and coupling constants. However, the photon distribution around an electron — which in light-cone quantization arises from self-energy graphs — is a little different. First of all it is measurable (e.g. when a charged particle traverses matter and looses energy[12,13]). It also has a classical interpretation in terms of the electric field of the fast moving electron, which almost looks like the electro-magnetic field of photons. Furthermore it is a function (albeit cutoff dependent, or — in the classical picture — dependent on the e^--radius). Fortunately, this function does not (to leading order α) depend on the electron energy or momentum — except via trivial kinematical factors.

We will now address the aspect of rotational invariance of the photon distribution in positronium. The photon distributions are IR-divergent for small x only ($G^{tot}_{k_\perp fixed} \stackrel{x\to 0}{\longrightarrow} \frac{1}{x}$), whereas there is no such effect for small $k_\perp$, i.e. in the trans-

verse direction. The mere fact, that $G(x, k_\perp)$ is IR-divergent should not come as a surprise, since the photon is massless and one expects that each electron is surrounded by an infinite number of soft photons.[#15] What might be surprising is the rotational asymmetry of the IR behaviour. In the following this effect will be investigated in some detail for a single electron, where one finds

$$G_{e^-}^{tot}(x, k_\perp) dx d^2k_\perp \propto \left(\frac{k_\perp}{x}\right)^2 \frac{x k_\perp dx\, dk_\perp}{\left[k_\perp^2 + (2mx)^2\right]^2}. \tag{43}$$

This should be compared with the soft component of the distribution function of a massless scalar boson around a fermion in a Yukawa theory

$$G_{Yuk}^{tot}(x, k_\perp) dx d^2k_\perp \propto \frac{x k_\perp dx\, dk_\perp}{\left[k_\perp^2 + (2mx)^2\right]^2}, \tag{44}$$

where the IR-divergence in the x and the $k_\perp$ directions are the same. In order to investigate the difference between photons and massless scalars in more detail, one can approximate the electromagnetic current j^μ, for small momentum transfers, by

$$j^\mu \approx \frac{e}{m} p^\mu, \tag{45}$$

where p^μ is the four momentum of the charged particle. Furthermore, in light-cone gauge, $\varepsilon^+ = 0$, $\varepsilon^\perp = 1$, $\varepsilon^- = \frac{k_\perp}{k^+}$, i.e. the matrix element for the emission of a soft photon

$$|M| \propto |j_\mu \varepsilon^\mu| \propto |\frac{p^+ k_\perp}{k^+}| = \frac{k_\perp}{x} \tag{46}$$

depends on the direction of the emitted photon. Actually, Eq.(46) is nothing but the familiar dipole formula and reflects that dipoles do not radiate along the dipole

#15 However, for fixed UV-cutoff, they carry only a finite momentum ($xG^{tot}(x)$ is still integrable). Thus the expansion in powers of α still makes sense.

axis. Applied to the field of a moving charge this implies that there should be a suppression for soft photons in the forward direction (or equivalently: photons with $\frac{k_\perp}{x} \to 0$).

5. Connection to QED Evolution

In atomic and molecular systems, interaction (intrinsic) photons (8) are important only for values of $x \sim \mathcal{O}(\alpha)$. Outside this soft regime they can in general be neglected compared to the self-energy (extrinsic) piece (7) (see also Fig. 2.) and it becomes a very good approximation to keep only the extrinsic component of the photon distributions. To leading order in α this is equivalent to performing 1^{st} order QED evolution similar to the well known QCD evolution[16] . From the point of view of the evolution equations, the interaction photons correspond to recombination processes (as discussed in Ref. 4 in the context of QCD) and can, for fixed values of x, be neglected in the limit $\Lambda_\perp \to \infty$. However, since we are working at finite (though large) $\Lambda_\perp$, there will always be a range of values of x where these recombination processes become important.#16 A rough estimate, where interaction photons become necessary, can be obtained as follows: for $x \to 0$, the total (extrinsic + intrinsic) momentum density of photons approaches its finite (for fixed cutoff) maximum value (12) $xG^{total}(x)\big|_{x=0} = \frac{2\alpha}{\pi} \log{(\Lambda_\perp r_\perp)^2}$. For those values of x, where xG^{self} alone exceeds this value, namely for

$$x < x_{Bohr} \approx \frac{1}{2mr_\perp}, \tag{47}$$

the interaction photons start to become relevant and emerge from the "noise". However, it is not until

$$x < x_{soft} \approx \frac{1}{2m\Lambda_\perp r_\perp^2} \tag{48}$$

the $xG^{self}(x)$ exceeds $2xG^{total}(x)\big|_{x=0}$ and interaction photons become essential

#16 In fact, in positronium, screening or recombination processes modify the leading behaviour for $x \to 0$.

to prevent $xG(x)$ from blowing up. For positronium with $r_\perp \approx m\alpha$ one finds $x_{Bohr} \approx \alpha$ and, with a typical cutoff of $\Lambda_\perp = m$, $x_{soft} \approx \alpha^2$.

In QCD similar processes are expected to screen the perturbative component of the gluon distribution at small x. However, there the non-abelian gluon-gluon interaction has to be taken into account which leads to different estimates of the soft gauge-field distributions.[4] Nevertheless, it is interesting to insert typical "hadronic" values ($m = \frac{1}{3}GeV$, $\Lambda_\perp = 2GeV$, $r_\perp = .5fm$) for the parameters in Eqs.(47) and (48), yielding $x_{Bohr} \approx 0.6$ and $x_{soft} \approx 0.15$ respectively.

6. Summary and Conclusions

We have studied the parton distributions in the weak coupling limit of QED. There is scaling as a function of the coupling in the sense that the fermion and boson distributions depend on Bjorken-x and the QED coupling α only through the ratio $\frac{x}{\alpha}$. Although they are the leading order in α solutions to a relativistic quantum field theory one can express these distributions in terms of the nonrelativistic Schrödinger wave functions. This is possible because, for small α, the motion of the charges in the rest frame becomes nonrelativistic.

We have derived general formulae to evaluate the leading order α photon distributions from the Schrödinger wave functions. In addition, in the Appendix A, we computed explicitly the photon distributions for the $n = 1, l = 0$ and $n = 2, l = 0, 1$ positronium states analytically. On the one hand, this is very helpful in generating an intuitive understanding about various relations between different effects. For example, it is possible to relate the transverse size of the positronium states and the soft component of the photon distribution (see Eq.(12)). Furthermore, there emerges an interesting connection between the longitudinal size of the $l = 1, l_z = 0$

state and an enhancement of the photon distribution for the wavelength which matches this size. These explicit positronium results can serve as a benchmark to test the accuracy of numerical calculations[7,5,8] for positronium by allowing α to become small.

For small α the momentum carried by the photons is proportional to the energy stored in the electric field. This has important consequences when two atoms (or two small molecules) bind together. The binding implies a decrease in the electric field energy, i.e. in molecules the virtual photons will always carry a smaller fraction of the total momentum than in the fragments. This result holds independent of the number of transverse dimensions (as long as $D_\perp < 3$), i.e. even in a regime ($D_\perp \leq 1$) where the QED interactions confine charged particles.

It would be interesting to investigate whether the relation between energy stored in the gauge field and the momentum carried by the gauge bosons can be generalized to non-abelian QCD. For weakly coupled Υ systems the weak coupling QED results immediately carry over to QCD but this should be considered as almost trivial, since the equations for weakly coupled $b\bar{b}$ are formally similar to the corresponding positronium equations. For the more interesting case — strongly coupled light quarks — the situation is less clear. But let us speculate for the moment what would happen if the momentum sum rule would carry over. Essentially this would mean that gluons would carry less of the momentum of a nucleus than of a nucleon. Detecting such an effect would be quite challenging because the size of the expected effect (typically the ratio between nuclear binding energies and nucleon masses or the QCD scale) would range at the few per cent level. It is not clear whether the shadowing observed in the data is related to these phenomena. Supposedly, there will be a difficulty in disentangling the two phenomena for the

following reason: the usual methods to extract the momentum of the gluons — measuring the momentum of the quarks and subtracting the result from one — introduce a systematic error from shadowing into the problem. Typically, one undercounts the momentum of the quarks in a nucleus because of this effect, i.e. one tends to associate more momentum to the gluons in a nucleus than they actually carry.

In addition to the decrease of the total gluon momentum other nuclear effects are conceivable. For example, the overlap of two nucleons would allow hidden color states and new gluon modes, with a wavelength that matches the separation of the di-nucleon, thus giving rise to a hump at small x in the ratio of nucleus versus nucleon gluon distribution. It would be interesting to compute the photon distribution in a hydrogen or positronium[17] molecule in order to see whether such an effect does occur in QED and if it does to see whether it is at all of practically observable size.

Furthermore, there should be the familiar Fermi motion effect for $x \to 1$. Otherwise the field energy effect would suggest a general decrease of the gluon structure function in the nucleus.

Acknowledgements

I would like to acknowledge Stan Brodsky for many helpful discussions. I also thank R.Warner, A.Langnau, M.Kaluza and X.Ji for critical comments on the interpretation of some of the phenomena discussed in this article.

APPENDIX A

PARTON DISTRIBUTIONS FOR THE ENERGETICALLY LOWEST POSITRONIUM STATES

In the following, the main techniques developed in this article will be applied to specific positronium states. This will perhaps help to illustrate the physical meaning of the various relations and sum rules which were derived in the main text. Furthermore, and this will be of particular importance for gaining an intuitive understanding, special emphasis will be put on the connections between the shape of the photon distribution function and the corresponding electron-positron wavefunctions and distribution functions.

The starting point is the coordinate space wavefunctions for positronium, which can be found in most textbooks on elementary quantum mechanics:[18]

$$\psi_{1s}(\vec{r}) \propto \exp(-\frac{m\alpha r}{2}) \tag{A.1}$$

$$\psi_{2s}(\vec{r}) \propto \left(1 - \frac{m\alpha r}{4}\right) \exp(-\frac{m\alpha r}{4}) \tag{A.2}$$

$$\psi_{2p\pm1}(\vec{r}) \propto (x \pm iy) \exp(-\frac{m\alpha r}{4}) \tag{A.3}$$

$$\psi_{2p0}(\vec{r}) \propto z \exp(-\frac{m\alpha r}{4}) \tag{A.4}$$

(up to a normalization constant). Upon taking the Fourier transform of the densities $|\psi(\vec{r})|^2$ one arrives at the form factors

$$F_A(\vec{q}) = \frac{1}{2} \int d^3\vec{k} \psi_A^*(\vec{k} + \vec{q}) \psi_A(\vec{k}) + c.c. \tag{A.5}$$

which are necessary for the computation of the photon distributions. One finds

$$F_{1s}(\vec{q}) = \frac{(\alpha m)^4}{[\vec{q}^2 + (\alpha m)^2]^2} \tag{A.6}$$

$$F_{2s}(\vec{q}) = \frac{(\alpha m/2)^4}{[\vec{q}^2 + (\alpha m/2)^2]^2} \times \left\{ 2 - \frac{7(\alpha m/2)^2}{\vec{q}^2 + (\alpha m/2)^2} + \frac{6(\alpha m/2)^4}{[\vec{q}^2 + (\alpha m/2)^2]^2} \right\} \tag{A.7}$$

$$F_{2p\pm1}(\vec{q}) = \frac{(\alpha m)^6}{[\vec{q}^2 + (\alpha m/2)^2]^3} \times \left\{ 1 - \frac{3q_\perp^2}{\vec{q}^2 + (\alpha m/2)^2} \right\} \tag{A.8}$$

$$F_{2p0}(\vec{q}) = \frac{(\alpha m/2)^6}{[\vec{q}^2 + (\alpha m/2)^2]^3} \times \left\{ 1 - \frac{6q_z^2}{\vec{q}^2 + (\alpha m/2)^2} \right\}. \tag{A.9}$$

Upon insertion of these form factors into Eqs. (8),(9),one obtains

$$xG_{1s}^{int}(x) = -\frac{2\alpha}{\pi} \left\{ (1 + 2z_1) \ln\left(\frac{1+z_1}{z_1}\right) - 2 \right\} \tag{A.10}$$

$$xG_{2s}^{int}(x) = -\frac{2\alpha}{\pi} \left\{ (1 + 7z_2) \ln\left(\frac{1+z_2}{z_2}\right) - 7 + \frac{\frac{5}{2}}{1+z_2} + \frac{1}{[1+z_2]^2} \right\} \tag{A.11}$$

$$xG_{2p\pm1}^{int}(x) = -\frac{2\alpha}{\pi} \left\{ (1 + 9z_2 + 12z_2^2) \ln\left(\frac{1+z_2}{z_2}\right) - 12z_2 - 3 - \frac{\frac{1}{2}}{1+z_2} \right\} \tag{A.12}$$

$$\begin{aligned} xG_{2p0}^{int}(x) = -\frac{2\alpha}{\pi} \Bigg\{ & (1 + 3z_2) \ln\left(\frac{1+z_2}{z_2}\right) - 3 + \frac{\frac{1}{2}}{1+z_2} \\ & -6z_2 \left[(1 + 4z_2) \ln\left(\frac{1+z_2}{z_2}\right) - 4 + \frac{1}{1+z_2} + \frac{\frac{1}{6}}{[1+z_2]^2} \right] \Bigg\}, \end{aligned} \tag{A.13}$$

where $z_1 = \left(\frac{2x}{\alpha}\right)^2$ and $z_2 = \left(\frac{4x}{\alpha}\right)^2$. The resulting intrinsic photon distributions are displayed in Fig.1.

As one might have expected, $xG^{int}(x)$ is mostly negative.[#17] This reflects the screening of part of the electric field in the bound state. Also, from the momentum sum rule (28), one knows that $\int dx\, xG^{int}(x) < 0$. Among the examples in Fig.1 one has even $xG^{int}(x) < 0$ with the exception of the $2p0$ ($n = 2, l = 1, l_z = 0$) state, which has a peak around $\hat{x} = \frac{2x}{\alpha} \approx 0.3$ (Fig. 1b). The physical origin of this peak becomes clear if one looks at the electron distributions in the various states. With (3)

$$f(x) = 2m \int d^2k_\perp |\psi_{NR}(k_L, k_\perp)|^2 \tag{A.14}$$

where

$$k_L = 2m\left(x - \frac{1}{2}\right) \tag{A.15}$$

one finds

$$f_{1s}(x) = \frac{1}{6\pi\alpha}\left[\hat{x}^2 + \frac{1}{4}\right]^{-3} \tag{A.16}$$

$$f_{2s}(x) = \frac{1}{16\pi\alpha}\left\{\frac{1}{3}\left[\hat{x}^2 + \frac{1}{16}\right]^{-3} - \frac{1}{16}\left[\hat{x}^2 + \frac{1}{16}\right]^{-4} + \frac{1}{320}\left[\hat{x}^2 + \frac{1}{16}\right]^{-5}\right\} \tag{A.17}$$

$$f_{2p\pm1}(x) = \frac{1}{2560\pi\alpha}\left[\hat{x}^2 + \frac{1}{16}\right]^{-4} \tag{A.18}$$

$$f_{2p0}(x) = \frac{\hat{x}^2}{320\pi\alpha}\left[\hat{x}^2 + \frac{1}{16}\right]^{-5} \tag{A.19}$$

with $\hat{x} = \frac{2}{\alpha}\left(x - \frac{1}{2}\right)$. These electron (or positron) distributions are depicted in Fig. 3. Note that only the $2p, l_z = 0$ state has a node in the electron distribution.

#17 Of course, if one includes the extrinsic or self-energy component of the virtual photon cloud (10) the result is always positive (Fig.2).

In this state one will find the electron most of the time with momentum fraction $\hat{x}_{e^-} \approx \pm\frac{\Delta\hat{x}}{2}$ (and the positron at $\hat{x}_{e^+} \approx \mp\frac{\Delta\hat{x}}{2}$) where $\Delta\hat{x} \approx 0.25$ is the separation between the two humps in f_{2p0} (Fig. 3). When e^- and e^+ trade positions they have to exchange a virtual photon carrying the momentum difference; i.e. $\hat{x}_\gamma = \Delta\hat{x} \approx 0.25$ and one expects to find photons with this momentum strongly enhanced — in agreement with Fig. 1.

Our next point is the verification of the momentum sum rule (28). Integrating Eqs. (A.10)-(A.13)one finds

$$\int_0^\infty dx x G_{1s}^{int}(x) = -\frac{\alpha^2}{3} = \frac{4}{3}\frac{V_1}{2m} \tag{A.20}$$

$$\int_0^\infty dx x G_{2s}^{int}(x) = -\frac{\alpha^2}{12} = \frac{4}{3}\frac{V_2}{2m} \tag{A.21}$$

$$\int_0^\infty dx x G_{2p\pm1}^{int}(x) = -\frac{3\alpha^2}{40} = \frac{9}{10}\frac{4}{3}\frac{V_2}{2m} \tag{A.22}$$

$$\int_0^\infty dx x G_{2p0}^{int}(x) = -\frac{\alpha^2}{10} = \frac{6}{5}\frac{4}{3}\frac{V_2}{2m}, \tag{A.23}$$

where $V_n = 2E_n = -\frac{\alpha^2 m}{2n^2}$ has been used. For the (rotational invariant) s-states Eqs.(A.20) and (A.21) directly agree with the sum rule (28). Though the p states do not satisfy the momentum sum rule (28) individually (A.22) ,(A.23) the average over polarization states does, as can be verified upon using $\frac{9}{10} + \frac{6}{5} + \frac{9}{10} = 3$. This should not come as a surprise, since we had to assume rotational invariance in the derivation of Eq.(28), which is in general guaranteed only after averaging over all

l_z components. Physically the deviation between Eqs.(A.22) and (A.23) implies that photons carry more momentum in $2p \pm 1$ positronium than they do in $2p0$ positronium, although the potential energy is the same for these states. This result has a nice quasi-classical interpretation: consider a positronium state moving fast along the z-direction. As indicated in Fig.4 the $l_z = 0$ state is mostly aligned parallel to the z-axis whereas the $l_z = \pm 1$-states extended more in the xy-plane. Thus, for the $l_z = \pm 1$-states, an observer at rest will measure an electromagnetic field which is reminiscent of an electromagnetic wave whereas the $l_z = 0$ state gives only rise to a longitudinal field, which is furthermore suppressed compared to the transverse field because of the different Lorentz transformation properties (37)-(40). Thus one expects more photons (in the sense of equivalent quanta[12,13]) to be present in the case of the $l_z = \pm 1$-states — which is consistent with Eqs. (A.3), (A.4).[#18]

In the rest of the appendix the focus will be more on the small x region of the photon distributions. It can be easily read off from Eqs.(A.10)-(A.13), that intrinsic photon distributions scale like

$$xG^{int}(x) \stackrel{x \to 0}{\longrightarrow} -\frac{2\alpha}{\pi} \ln \frac{1}{x^2}. \tag{A.24}$$

A comparison with Eq.(7)shows that this scaling behaviour is — up to a sign — the same for an unbound e^+e^--pair. Hence the soft component of the total photon distribution is screened in a bound, neutral system — which is exactly what one would expect classically. As has been shown in section 2, the limit (12)

$$\lim_{x \to 0} x \left[G_A^{int}(x) - G_B^{int}(x) \right] = \frac{2\alpha}{\pi} \left[\langle \ln r_\perp^2 \rangle_A - \langle \ln r_\perp^2 \rangle_B \right] \tag{A.25}$$

#18 Please notice that $\langle x_\gamma^{int} \rangle < 0$, i.e. "more photons", which means $\langle x_\gamma^{total} \rangle_{2p\pm1} > \langle x_\gamma^{total} \rangle_{2p\pm1}$, implies $| \langle x_\gamma^{int} \rangle_{2p\pm1} | < | \langle x_\gamma^{int} \rangle_{2p\pm1} |$.

(where A and B are arbitrary positronium states) has a simple physical meaning: increasing the transverse extension of a state, the transverse electric field in the rest frame will extend over a larger volume, hence more soft photons will be present in the infinite momentum frame. A first estimate about the r.h.s. of Eq.(A.25) can be obtained by approximating

$$\langle \ln r_\perp^2 \rangle_A - \langle \ln r_\perp^2 \rangle_B \approx \ln \langle r_\perp^2 \rangle_A - \ln \langle r_\perp^2 \rangle_B \,. \tag{A.26}$$

The transverse radii can be easily extracted from the form factors (A.6)-(A.9), using

$$\langle r_\perp^2 \rangle_A = -4 \frac{d}{dq_\perp^2} F_A(\vec{q}), \tag{A.27}$$

which yields

$$\langle r_\perp^2 \rangle_{1s} = \frac{8}{(\alpha m)^2} \tag{A.28}$$

$$\langle r_\perp^2 \rangle_{2s} = \frac{112}{(\alpha m)^2} \tag{A.29}$$

$$\langle r_\perp^2 \rangle_{2p\pm1} = \frac{96}{(\alpha m)^2} \tag{A.30}$$

$$\langle r_\perp^2 \rangle_{2p0} = \frac{48}{(\alpha m)^2}. \tag{A.31}$$

Using Eq. (A.26) and inserting these transverse radii into Eq. (A.25) one can easily verify the pattern obtained in Fig.4 for $x \to 0$.[#19] Again one observes a significant difference for the various p-states caused by their different orientation.

#19 Of course one can also use the exact results for $\langle \ln r_\perp^2 \rangle$, which are (up to an overall additive constant) respectively 2, $\frac{7}{2} + \ln 4$, $\frac{7}{2} + \ln 4$, $\frac{5}{2} + \ln 4$, to verify the $x \to 0$ sum rule (A.25).

APPENDIX B

COMPARISON WITH RESULTS FROM MATRIX DIAGONALIZATION

In this Appendix the results from section 2 will be extended to rather small values of the transverse cutoff ($\Lambda_\perp = \mathcal{O}(M\alpha)$). In principle this will allow a comparison with numerical work on the positronium system[8]. However, in practice, this is not completely straightforward since these works are usually performed for rather large values of the coupling constant ($\alpha \approx 0.3$). First of all this means that our results have to be extended into a regime, where the approximations used (e.g. one-photon approximations, neglecting the binding in the energy denominator) become questionable. Secondly, it will be difficult to match the different cutoff procedures.

Fortunately, as far as the approximations are concerned, the simplifications used in Ref. 8 are rather similar to the ones applied here. Thus, even if the approximations are too crude for such large couplings, this will not disturb a direct comparison between this work and Ref. 8 . The second objection — the difficulties in matching cutoffs — will be more problematic.

We will now turn our attention to the computation of the photon distributions where relations similar to the ones used in section 2 and the Appendix A will be used. However, the cutoff $\Lambda_\perp$ will be kept finite throughout and terms of $\mathcal{O}(\left(\frac{M\alpha}{\Lambda_\perp}\right)^2)$ or $\mathcal{O}(\left(\frac{Mx}{\Lambda_\perp}\right)^2)$, which arise from the integrals, will no longer be discarded. Finite cutoff effects are most important in the self-interactions[(7)], where one finds

$$xG^{self}_{\Lambda_\perp}(x) = \frac{2\alpha}{\pi}\int_0^{\Lambda_\perp^2} dk_\perp^2 \frac{k_\perp^2}{\left[k_\perp^2+(2mx)^2\right]^2} + \mathcal{O}(\alpha^2)$$
$$= \frac{2\alpha}{\pi}\left[\log\left(\frac{\lambda+z}{z}\right) - \frac{\lambda}{\lambda+z}\right] \quad , \tag{B.1}$$

where $\lambda = \left(\frac{\Lambda_\perp}{m\alpha}\right)^2$ and $z = \left(\frac{2x}{\alpha}\right)^2$. Although a cutoff in the interaction piece is of minor importance (as long as $\Lambda_\perp > m\alpha$) the impact of $\Lambda_\perp < \infty$ in G^{int} on the $1s$ photon distribution will be demonstrated here

$$xG^{int}_{\Lambda_\perp,1s}(x) = \frac{2\alpha}{\pi}\int_0^{\Lambda_\perp^2} dk_\perp^2 \frac{k_\perp^2 F_{1s}(k_\perp^2+(xM)^2)}{\left[k_\perp^2+(2mx)^2\right]^2} + \mathcal{O}(\alpha^2)$$
$$= \frac{2\alpha}{\pi}\left\{(1+2z_1)\left[\log\left(\frac{z_1}{1+z_1}\right)+\log\left(1+\frac{1}{z_1+\lambda}\right)\right] + \frac{\lambda}{\lambda+z_1} + \frac{\lambda}{1+\lambda+z_1}\right\} \tag{B.2}$$

Before one can compare these analytic results for finite $\Lambda_\perp$ with the results from matrix diagonalization the cutoff conditions have to be matched. Here, a sharp cutoff on $k^2_{\perp\gamma}$ is imposed whereas Ref.8 uses the regularizing conditions

$$\frac{m^2+k^2_{\perp e^-}}{x_{e^-}(1-x_{e^-})} \leq 4m^2+\Lambda^2 \tag{B.3}$$

and

$$\frac{m^2+k^2_{\perp e^+}}{x_{e^+}(1-x_{e^+})} \leq 4m^2+\Lambda^2. \tag{B.4}$$

For weak coupling, where $x_{e^-} \approx x_{e^+} \approx \frac{1}{2}$, these conditions correspond to[#20]

$$k_{\perp\gamma} \leq \frac{\Lambda^2}{4}. \tag{B.5}$$

Following Ref.8 we use $\Lambda^2 = m^2$, hence $\Lambda_\perp^2 = \frac{m^2}{4}$ (Fig.5). A comparison with

#20 At least if one neglects $k_{\perp e^\pm}$ before the emission of the photon (see below) — which is justified, provided $\Lambda \gg M\alpha$.

Ref.8 shows that Eq.(B.5) yields too many photons and also a steeper slope (Fig. 5). This arises from the difference in the cutoff conditions for finite α and can be understood as follows. First of all, after emitting a photon of typically $x = 0.1$ to 0.2 an electron that had initially $x_{e^-} = 0.5$ will now carry only $x_{e^-} = 0.3$ to 0.4. Hence Eqs.(B.3),(B.4) no longer corresponds to Eq.(B.5) but rather $k_\perp^2 \leq (1-(2x_\gamma)^2)\left(m^2+\frac{\Lambda^2}{4}\right) - m^2$.#21

Secondly, for finite α, the initial $e^\pm$ (before emitting the photon) has in general already a nonzero value of $k_\perp$ ($\langle k_\perp^2 \rangle = \frac{m^2\alpha^2}{6}$). Ref.8 has a cutoff condition on $k_{\perp e^\pm}$ whereas the cutoff condition in this work is applied on $k_{\perp\gamma}$. The difference between these two conditions can be estimated using

$$\langle k_{\perp e^\pm}^2 \rangle_{e^+e^-\gamma} = \langle k_{\perp\gamma}^2 \rangle_{e^+e^-\gamma} + \langle k_{\perp e^\pm}^2 \rangle_{e^+e^-}\,, \tag{B.6}$$

where the momenta of the initial electron and the photon were assumed to be uncorelated and the nonrelativistic virial theorem (30) has been applied. Hence one should use $\Lambda_{\perp\gamma}^2 \approx \Lambda_{\perp e^\pm}^2 - \frac{m^2\alpha^2}{6}$. This effect results in a general suppression of photons for all x. Combining both effects one obtains the improved relation to transform the cutoff in Ref.8 into a transverse photon momentum cutoff

$$\Lambda_{\perp\gamma}^2 = (1-(2x_\gamma)^2)\left(m^2+\frac{\Lambda^2}{4}\right) - m^2\left(1+\frac{\alpha^2}{6}\right). \tag{B.7}$$

When inserted into Eqs.(B.1) and (B.2) the agreement with the matrix diagonalization result improves considerably (Fig.5).

#21 This explains in particular the difference of the slopes in Fig.5.

REFERENCES

1. C.Scholz (NMC), private discussion; R.Peccei, Invited Lectures, SLAC Summer Institute, 1991.
2. E.L.Berger and D.Jones, Phys.Rev.D23(1981) 1521; P.Kalyniak, M.K.Sundaresan and P.J.S.Watson, Phys.Lett.216B (1989) 397.
3. S.J.Brodsky and J.F.Gunion, Phys.Rev.D19 (1979)1005; S.J.Brodsky and I.Schmidt, Phys.Lett.234B (1990) 144.
4. L.V.Gribov, E.M.Levin and M.G.Ryskin, Nucl.Phys.B188 (1981) 555; A.H.Mueller and J.Qiu, Nucl.Phys.B268 (1986) 427; F.E.Close and J.Qiu, Phys.Rev.D40 (1989) 2820; J.Collins and J.Kwiecinski, Nucl.Phys. B335 (1990) 89.
5. A.C.Tang, S.J.Brodsky and H.-C.Pauli, to be published in Phys.Rev.D .
6. D.Mustaki, S.Pinsky, J.Shigemitsu and K.Wilson, to be published in Phys.Rev.D.
7. M.Krautgärtner, H.-C.Pauli and F.Wölz, preprint, MPIH-V4-1991; L.C.L.Hollenberg, K.Higashima, R.C.Warner and B.H.J.McKellar, preprint, KEK-TH-280.
8. M.Kaluza and H.-C.Pauli, preprint MPIH-??-1991.
9. S.J.Brodsky and H.-C.Pauli, Invited Lectures, Schladming, 1991, SLAC-PUB-5558.
10. S.J.Brodsky and G.P.Lepage, Phys.Rev.D22 (1980) 2157.
11. M.Burkardt and A.Langnau, to be published in Phys.Rev.D; M.Burkardt and A.Langnau, submitted to Phys.Rev.D.
12. E.Fermi, Zeitschr.f.Phys.29 (1924) 315; E.J.Williams, Proc.Roy.Soc.London (A)139 (1933) 163.
13. L.D.Landau and E.M.Lifschitz, "Quantum Electrodynamics", Oxford, Eng., Pergamon Press,1982.

14. J.D.Jackson, "Classical Electrodynamics", New York, Wiley, 1975.

15. R.P.Feynman, R.D.Leighton and M.Sands, "The Feynman Lectures on Physics", Reading, Massachusetts, Addison-Wesley, 1963.

16. V.N.Gribov and I.N.Lipatov, Sov.J.Nucl.Phys.15 (1972) 438; G.Altarelli and G.Parisi, Nucl.Phys.B126 (1977) 298.

17. M.A.Abdel-Raouf, Fortschr.Phys.36 (1988) 521.

18. J.J.Sakurai, "Modern Quantum Mechanics", Addison-Wesley, 1985.

Figure Caption

*Fig.*1 a.) Intrinsic photon distribution for the $1s$, $2s$ and the $2p$ states (A.10)-(A.13). The logarithmic growth for $x \to 0$ is cancelled by the extrinsic contribution.

b.) same as a.) but using a different scale on the ordinate.

*Fig.*2 Total photon distribution (10) for the four lightest positronium states ($\alpha = \frac{1}{137}$, $\Lambda_\perp = m$). The result is compared to the extrinsic distribution (7) for the same parameters.

*Fig.*3 Electron distribution functions, Eqs.(A.16)- (A.19), for the $n = 1, 2$ positronium states (only valence component).

*Fig.*4 Schematic representation of the spatial orientation of the $l_z = \pm 1$ and $l_z = 0$ states and the resulting electric field. The extensions of the orbitals reflect actual longitudinal and transverse proportions (A.30),(A.31).

*Fig.*5 Finite cutoff results for the (total) photon distribution in the ground state of positronium, using $\alpha = 0.3$. Compared are (i) the calculations with $\Lambda_\perp^2 = \frac{m^2}{4}$ (B.5) with (ii) the improved cutoff Eq.(B.7) . The squares are numerical results from Ref.8 .

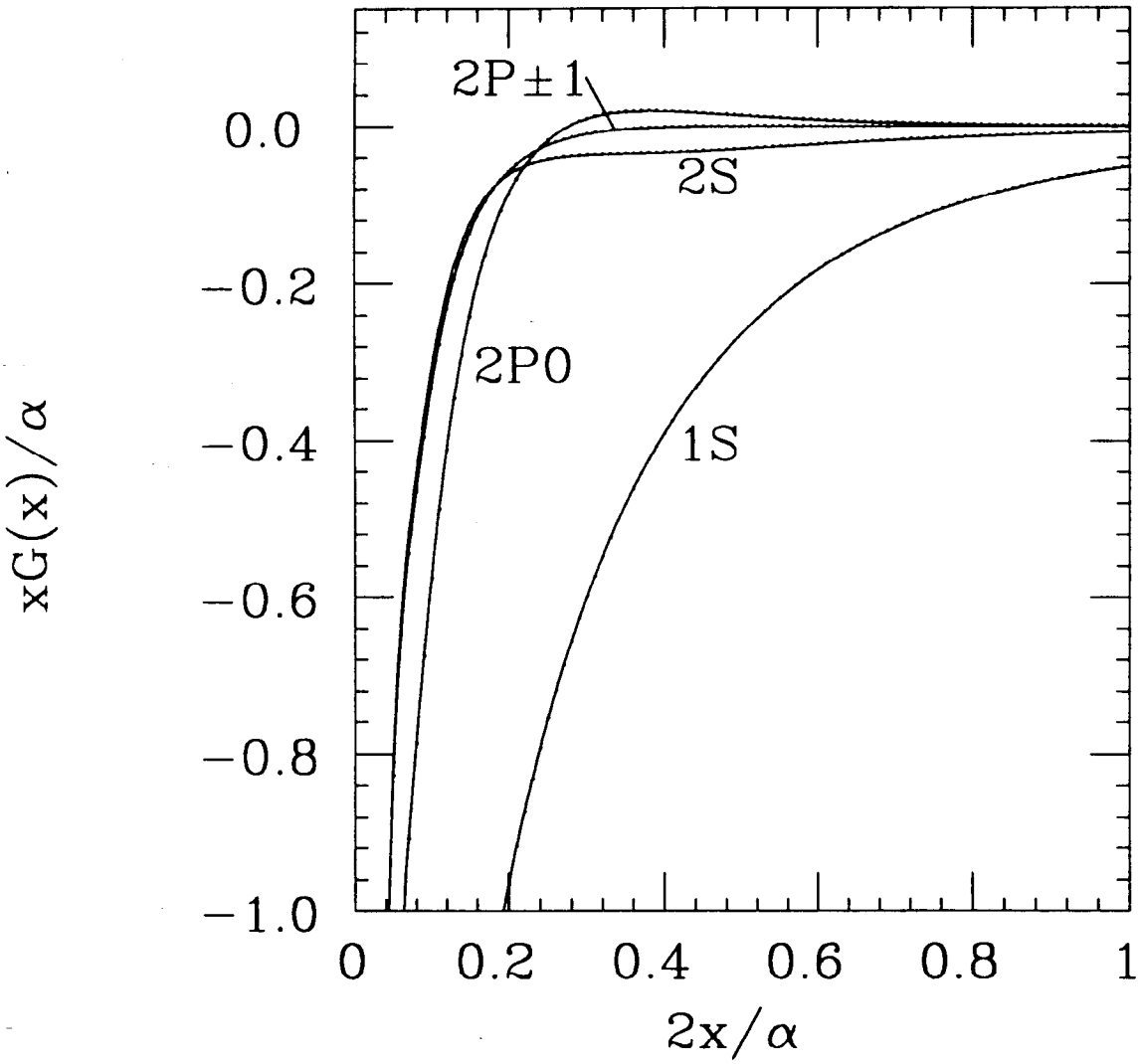

Fig. 1a

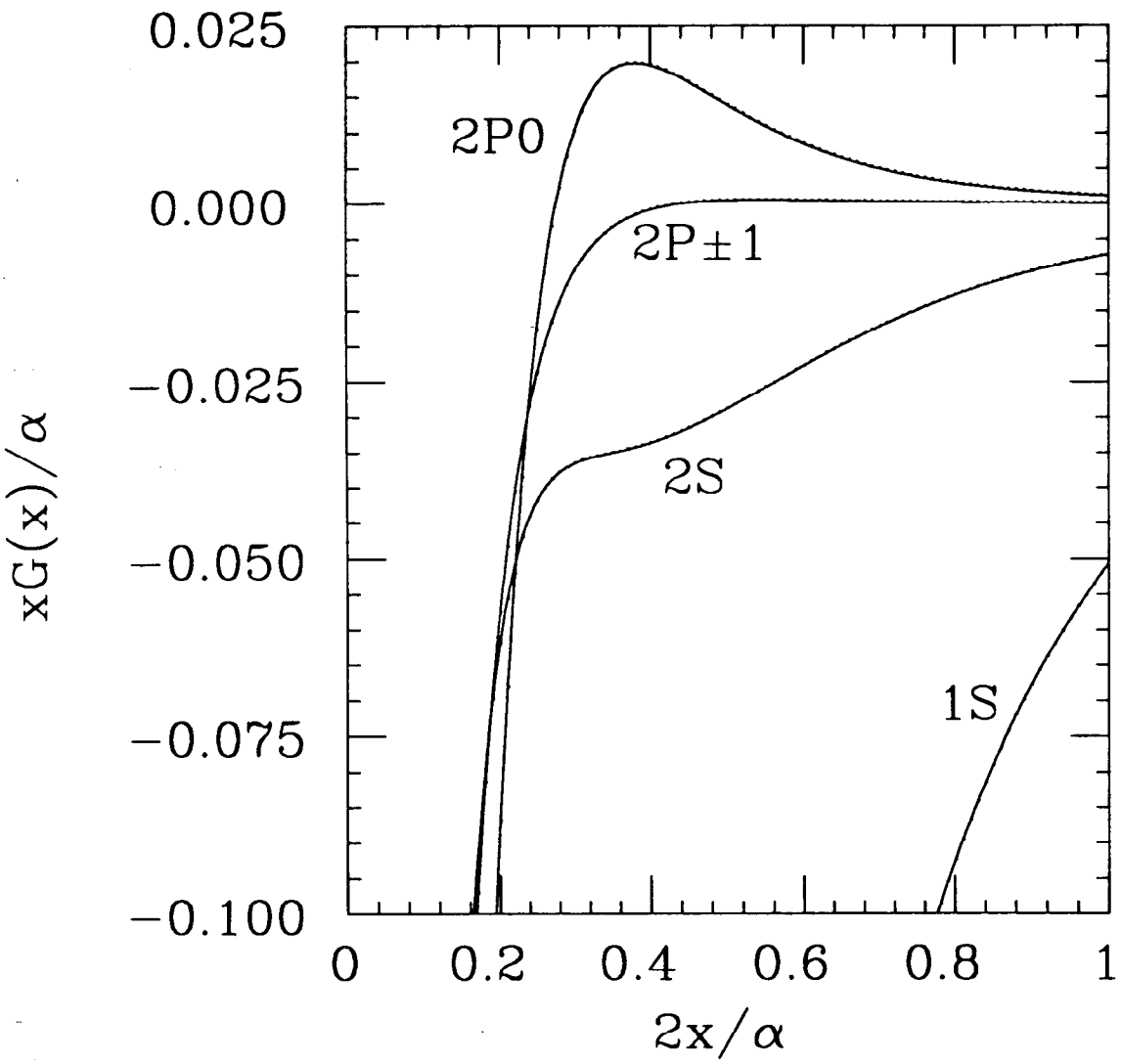
0.025
0.000
−0.025
−0.050
−0.075
−0.100
xG(x)/α
2P0
2P±1
2S
1S
0
0.2
0.4
0.6
0.8
1
2x/α

Fig. 1b

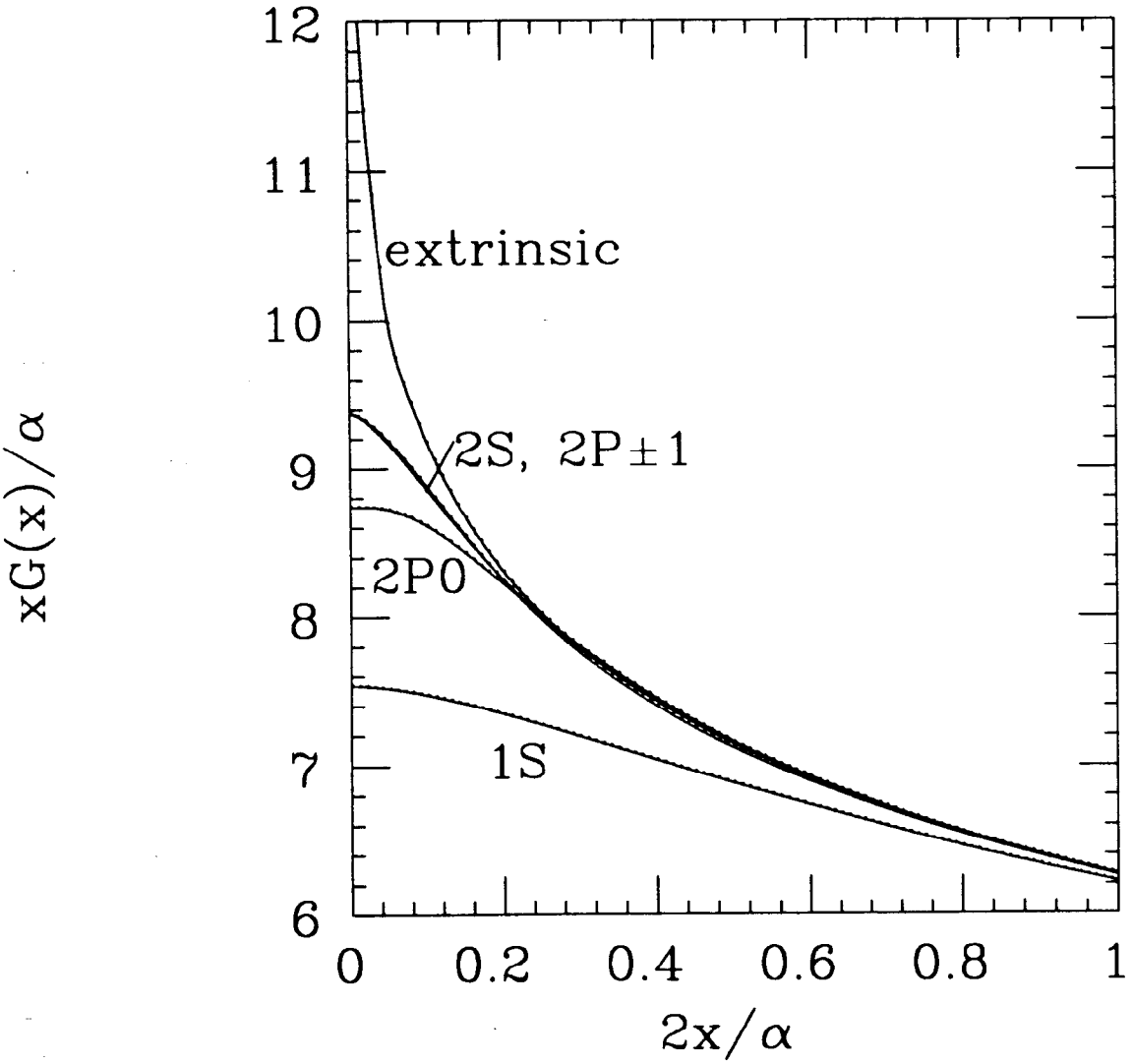

Fig. 2

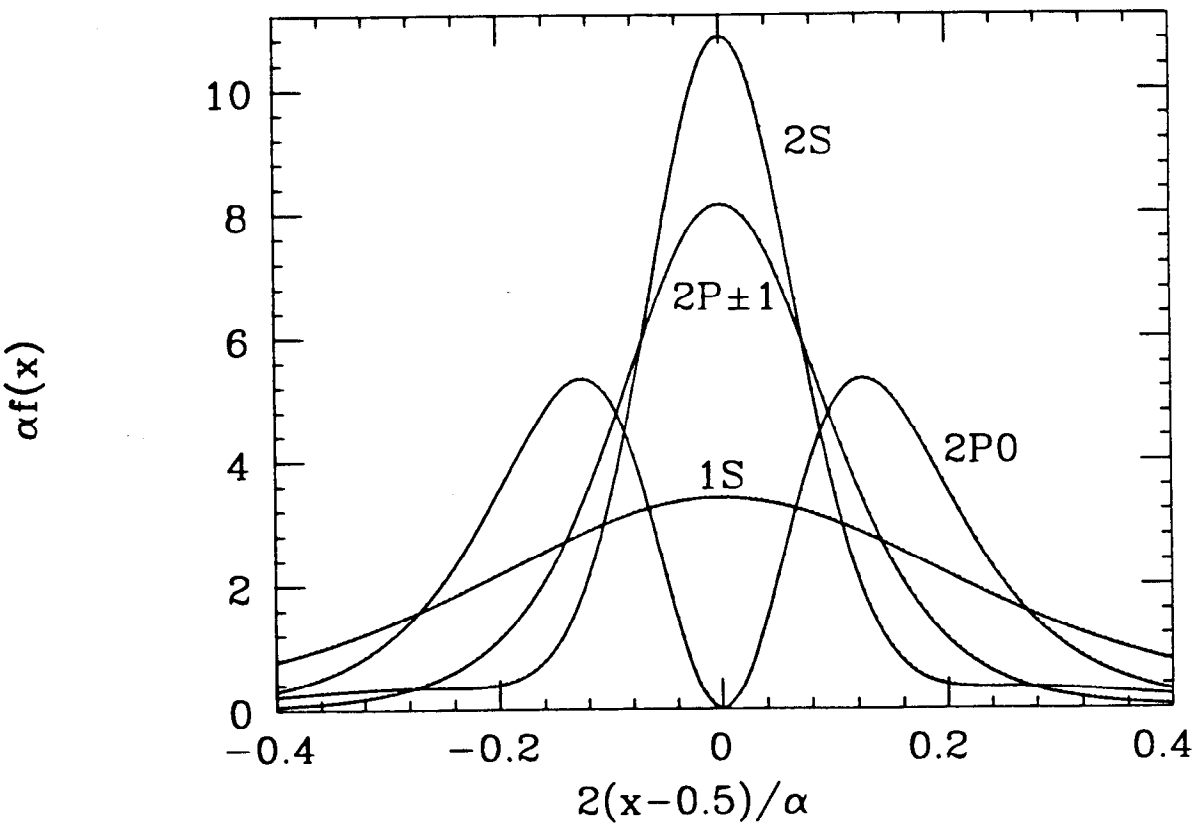

Fig. 3

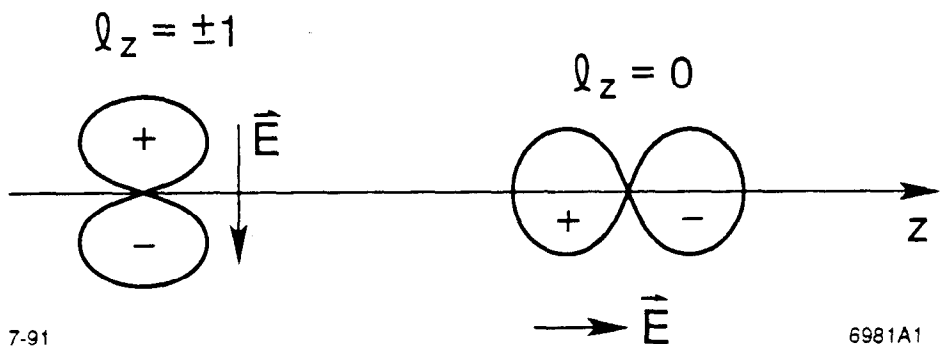

Fig. 4

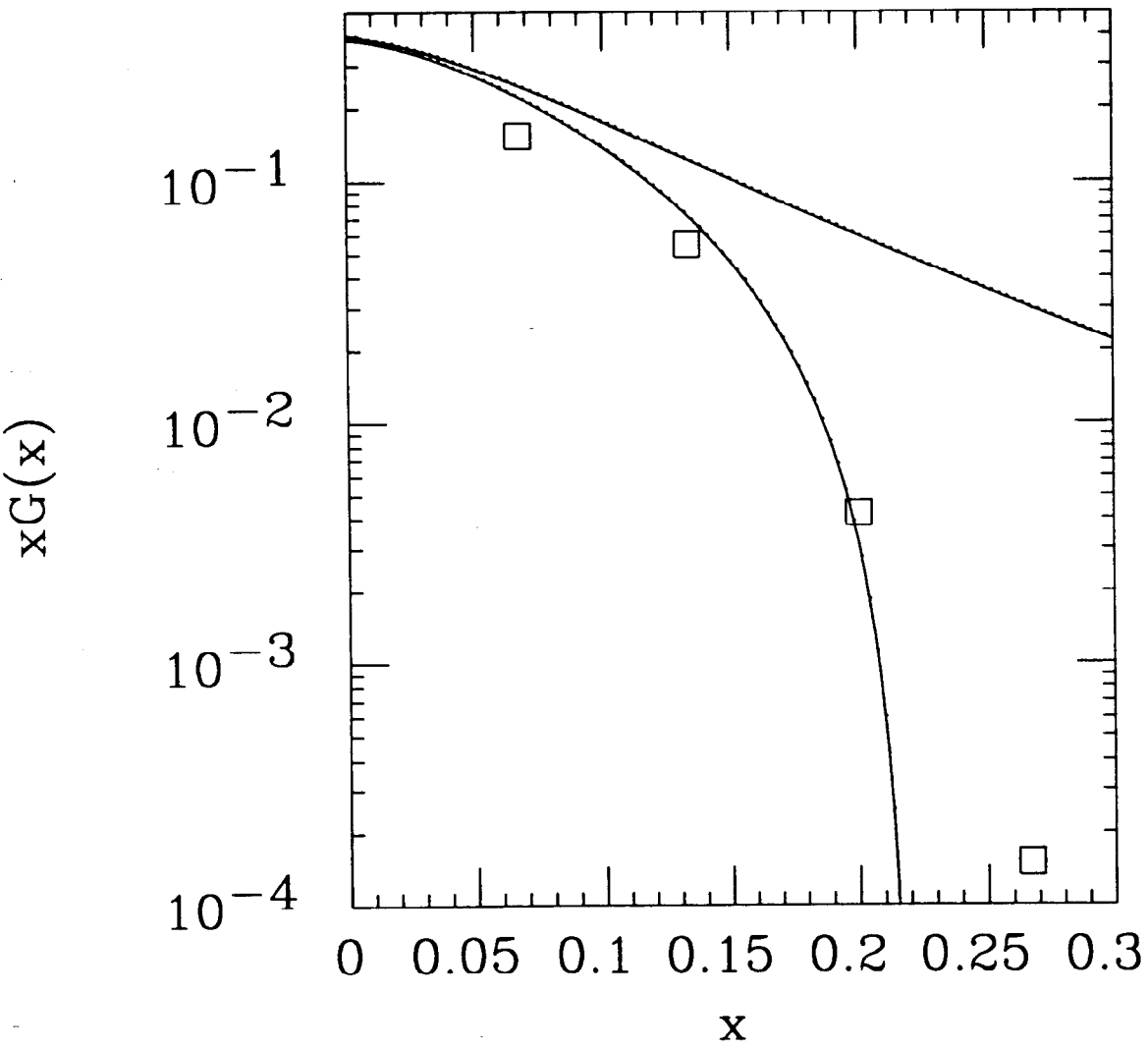

Fig. 5